DEVELOPMENT AND APPLICATION OF BENCHMARK EXAMPLES FOR MIXED-MODE I/II QUASI-STATIC DELAMINATION PROPAGATION PREDICTIONS

Ronald Krueger

ABSTRACT

The development of benchmark examples for quasi-static delamination propagation prediction is presented. The example is based on a finite element model of the Mixed-Mode Bending (MMB) specimen for 50% mode II. The benchmarking is demonstrated for Abaqus/Standard®, however, the example is independent of the analysis software used and allows the assessment of the automated delamination propagation prediction capability in commercial finite element codes based on the virtual crack closure technique (VCCT). First, a quasi-static benchmark example was created for the specimen. Second, starting from an initially straight front, the delamination was allowed to propagate under quasi-static loading. Third, the load-displacement as well as delamination length versus applied load/displacement relationships from a propagation analysis and the benchmark results were compared, and good agreement could be achieved by selecting the appropriate input parameters. The benchmarking procedure proved valuable by highlighting the issues associated with choosing the input parameters of the particular implementation. Overall, the results are encouraging, but further assessment for mixed-mode delamination fatigue onset and growth is required.

INTRODUCTION

Over the past two decades, the use of fracture mechanics has become common practice to characterize the onset and growth of delaminations. In order to predict delamination onset or growth, the calculated strain energy release rate components are

*R. Krueger, National Institute of Aerospace, 100 Exploration Way, Hampton, VA, 23666, resident at Durability, Damage Tolerance and Reliability Branch, MS 188E, NASA Langley Research Center, Hampton, VA, 23681, USA.

compared to interlaminar fracture toughness properties measured over a range from pure mode I loading to pure mode II loading.

The virtual crack closure technique (VCCT) is widely used for computing energy release rates based on results from continuum (2D) and solid (3D) finite element (FE) analyses and to supply the mode separation required when using the mixed-mode fracture criterion [1, 2]. The virtual crack closure technique was recently implemented into several commercial finite element codes such as Abaqus/Standard®[1], MD Nastran™[2], Marc™[2] and ANSYS[3]. As new methods for analyzing composite delamination are incorporated into finite element codes, the need for comparison and benchmarking becomes important since each code requires specific input parameters unique to its implementation. These parameters are unique to the numerical approach chosen and do not reflect real *physical* differences in delamination behavior.

An approach for assessing the mode I, mode II and mixed-mode I and II, delamination propagation capabilities in commercial finite element codes under static loading was recently presented and demonstrated for VCCT for ABAQUS® [3,4] as well as MD Nastran™ and Marc™ [5]. First, benchmark results were created manually for finite element models of the mode I Double Cantilever Beam (DCB), the mode II End Notched Flexure (ENF) and the mixed-mode I/II Single Leg Bending (SLB) specimen. Second, starting from an initially straight front, the delamination was allowed to propagate using the automated procedure implemented in the finite element software. The approach was then extended to allow the assessment of the delamination fatigue growth prediction capabilities in commercial finite element codes [4,6].

The objective of the present study was to create additional benchmark examples to simulate mixed-mode I/II conditions based on the Mixed-Mode Bending (MMB) specimen shown in Figure 1. Static benchmark results were created for three mixed-mode ratios (G_{II}/G_T =0.2, 0.5, and 0.8) based on the approach developed earlier [3].

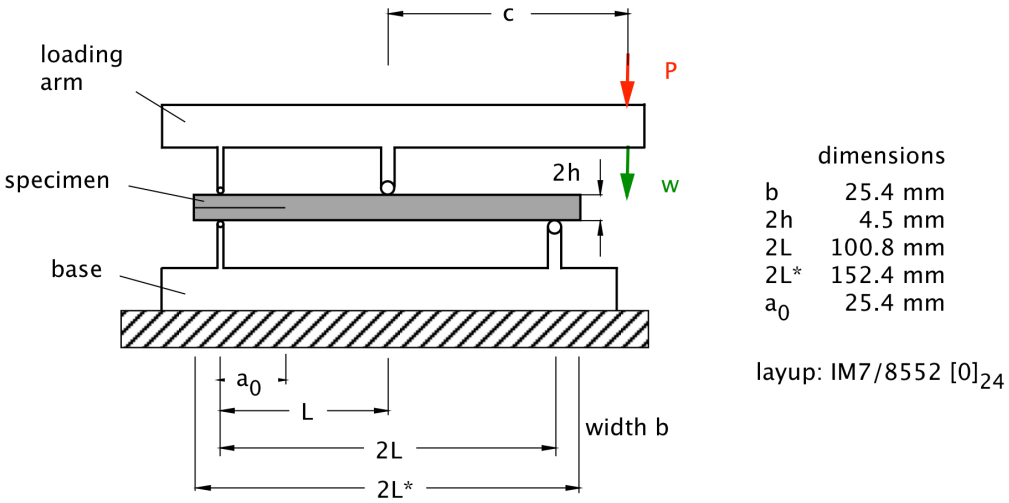

Figure 1. *Mixed-Mode Bending (MMB) Specimen.*

[1] ABAQUS® is a product of Dassault Systèmes Simulia Corp. (DSS), Providence, RI, USA
[2] MD Nastran™ and Marc™ are manufactured by MSC.Software Corp., Santa Ana, CA, USA. NASTRAN® is a registered trademark of NASA.
[3] ANSYS® is a product of ANSYS, Inc., Canonsburg, PA, USA

To create the benchmark results, two-dimensional finite element models were used for simulating the MMB specimens with different delamination lengths a_0. For each delamination length modeled, the load, P, and the displacement, w, were monitored. The total strain energy release rate, G_T, and mixed-mode ratio, G_{II}/G_T, were calculated for a fixed applied displacement. The delamination was assumed to propagate when the computed energy release rate, G_T, reaches the mixed-mode fracture toughness G_c. Thus, critical loads and critical displacements for delamination propagation were calculated for each delamination length modeled. From these critical load/displacement results, benchmark solutions were created. It is assumed that the load/displacement relationship computed during automatic propagation should closely match the benchmark cases.

After creating the benchmark cases, the approach was demonstrated for the commercial finite element code Abaqus/Standard®. Starting from an initially straight front, the delamination was allowed to propagate under quasi-static loading based on the algorithms implemented into the software. Input control parameters unique to Abaqus/Standard® were varied to study the effect on the computed delamination propagation. These parameters included the release tolerance and stabilization factors as discussed later. The benchmark enabled the selection of the appropriate input parameters that yielded good agreement between the results obtained from the propagation analysis and the benchmark results. Once the parameters have been identified, they may then be used with confidence to model delamination growth for more complex configurations.

In this paper, only the development of one benchmark case (G_{II}/G_T =0.5) for the assessment of the quasi-static delamination propagation is presented. Examples of automated propagation analyses are shown, and the selection of the required code specific input parameters are discussed. More detailed information about the other two benchmark cases for mixed-mode ratios G_{II}/G_T =0.2 and 0.8 may be found in reference 7.

METHODOLOGY BASED ON FRACTURE MECHANICS

For the current numerical investigation, the Mixed-Mode Bending (MMB) specimen, as shown in Figure 1, was chosen since it is simple, and exhibits the mixed-mode I/II opening fracture mode over a wide range of mixed-mode ratios G_{II}/G_T. For this paper, only results from finite element models for one mixed-mode ratios (G_{II}/G_T =0.5) are discussed. Fracture mechanics concepts [8], were applied to the MMB specimen to create the benchmark example. For the current study, MMB specimens made of IM7/8552 graphite/epoxy with a unidirectional layup, $[0]_{24}$, were modeled. The material, layup, overall specimen dimensions including initial crack length, a_0, were identical to specimens used in related experimental studies [9]. The material properties are given in Table I.

TABLE I. MATERIAL PROPERTIES [7].

E_{11} = 161 GPa	E_{22} = 11.38 GPa	E_{33} = 11.38 GPa
ν_{12} = 0.32	ν_{13} = 0.32	ν_{23} = 0.45
G_{12} = 5.2 GPa	G_{13} = 5.2 GPa	G_{23} = 3.9 GPa

A quasi-static mixed-mode fracture criterion is determined by plotting the interlaminar fracture toughness, G_c, versus the mixed-mode ratio, G_{II}/G_T as shown in Figure 2. The fracture criterion is generated experimentally using pure Mode I (G_{II}/G_T=0) Double Cantilever Beam (DCB) tests, pure Mode II (G_{II}/G_T=1) End-Notched Flexure (ENF) tests [9], and Mixed Mode Bending (MMB) tests of varying ratios of G_I and G_{II}. For the material used in this study, the experimental data (open symbols) and mean values (filled symbols) are shown in Figure 2. A 2D fracture criterion was suggested by Benzeggah and Kenane [10] using a simple mathematical relationship between G_c and G_{II}/G_T

$$G_c = G_{Ic} + (G_{IIc} - G_{Ic}) \left(\frac{G_{II}}{G_T}\right)^{\eta} \quad (1)$$

In this expression, typically called B-K criterion, G_{Ic} and G_{IIc} are the experimentally determined fracture toughness data for mode I and II as shown in Figure 2. The exponent η was determined by a curve fit using the Levenberg-Marquardt algorithm in the KaleidaGraph™ graphing and data analysis software [11]. The parameters G_{Ic}, G_{IIc} and η are required input to perform a VCCT analysis in Abaqus/Standard®, as discussed in detail in reference 7.

During an automated propagation analysis, the total strain energy release rate, G_T, and the mixed-mode ratio G_{II}/G_T are computed using VCCT. The failure index, G_T/G_c, is calculated by correlating the computed total energy release rate, G_T, with the mixed-mode fracture toughness, G_c, of the graphite/epoxy material. As shown in equation (1), the mixed-mode fracture toughness, G_c, is a function of the mixed-mode ratio G_{II}/G_T (see also Figure 2). It is assumed that the delamination propagates when the failure index, G_T/G_c, reaches unity.

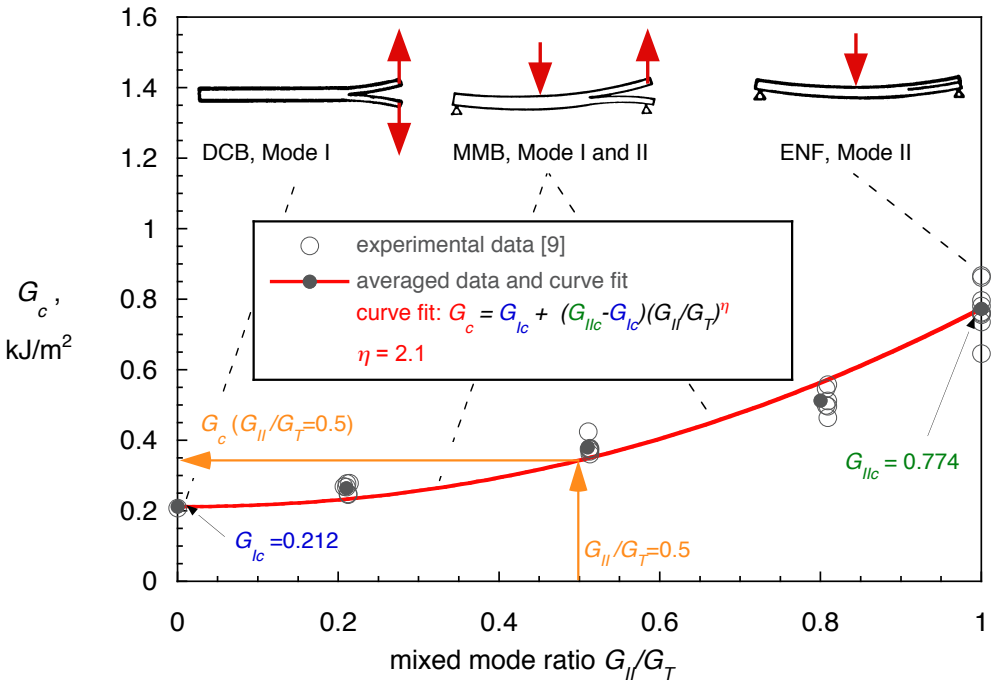

Figure 2. *Mixed mode fracture criterion for IM7/8852.*

FINITE ELEMENT MODELING

Model description

An example of a two-dimensional finite element model of a Mixed-Mode Bending (MMB) specimen with boundary conditions is shown in Figure 3 for a mixed-mode ratio G_{II}/G_T =0.5. Based on previous experience [3,4,6], the specimen was modeled with solid plane strain elements (CPE4I) in Abaqus/Standard® 6.10. Along the length, all models were divided into different sections with different mesh refinement as shown in Figure 3a. The MMB specimen was modeled with six elements through the specimen thickness (*2h*) as shown in the detail of Figure 3b. The resulting element length at the delamination tip was Δa=0.5 mm. The load apparatus was modeled explicitly using rigid beam elements (R2D2) as shown in Figure 3a. Multi-point constraints were used to connect the rigid elements with the planar model of the specimen and enforce the appropriate boundary conditions as shown in Figures 3b and c.

The plane of delamination was modeled as a discrete discontinuity in the center of the specimen. For the analysis in Abaqus/Standard® 6.10, the models were created as separate meshes for the upper and lower part of the specimens with identical nodal point coordinates in the plane of delamination [12]. Two surfaces (top and bottom surface) were defined to identify the contact area in the plane of delamination as shown in Figures 3b and c. Additionally, a node set was created to define the intact (bonded nodes) region.

An example of a three-dimensional finite element models of the MMB specimen is shown in Figure 4. Along the length, all models were divided into different sections with different mesh refinement. A refined mesh was used in the center of the MMB specimen as shown in the detail of Figure 4b. Across the width, a uniform mesh (25 elements) was used to avoid potential problems at the transition between a coarse and finer mesh [3-6]. Through the specimen thickness (*2h*), six elements were used as shown in the detail of Figure 4b. The resulting element length at the delamination tip was Δa=0.5 mm. The specimen was modeled with solid brick elements (C3D8I), which had yielded excellent results in previous studies [3,4,6]. The load apparatus was modeled explicitly using rigid plate elements (R3D4) as shown in Figure 4a. As before for the two-dimensional model, multi-point constraints were used to connect the rigid elements with the solid model of the specimen and enforce the appropriate boundary conditions.

Static delamination propagation analysis

For the automated delamination propagation analysis, the VCCT implementation in Abaqus/Standard® 6.10 was used. The plane of delamination in three-dimensional analyses is modeled using the existing Abaqus/Standard® crack propagation capability based on the contact pair capability [12]. Additional element definitions are not required, and the underlying finite element mesh and model does not have to be modified [12]. The implementation offers a crack and delamination propagation capability in Abaqus/Standard®. During the analysis, the energy release rate at the crack tip is calculated at the end of a converged increment. Once the energy release rate exceeds the critical strain energy release rate (including the user-specified mixed-

mode criteria as shown in Figure 2), the node at the crack tip is released in the following increment, which allows the crack to propagate. To avoid sudden loss of numerical stability when the crack tip is propagated during the analysis, the force at the crack tip is released gradually during succeeding increments. The release is performed in such a way that the force is brought to zero before the next node along the crack path begins to open [12,13].

In addition to the mixed-mode fracture criterion, Abaqus/Standard® requires additional input for the propagation analysis using VCCT. If a user specified release tolerance is exceeded in an increment $(G\text{-}G_c)/G_c > release\ tolerance$, a cutback operation is performed which reduces the time increment. In the new smaller increment, the strain energy release rates are recalculated and compared to the user specified release tolerance. The cutback reduces the degree of overshoot and improves the accuracy of the local solution [12]. A release tolerance of 0.2 is suggested in the handbook [12]. To help overcome convergence issues during the propagation analysis, Abaqus/Standard® provides:

- *contact stabilization* that is applied across only selected contact pairs and used to control the motion of two contact pairs while they approach each other in multi-body contact. The damping is applied when bonded contact pairs debond and move away from each other [12.13]
- *automatic, or static, stabilization* that is applied to the motion of the entire model and is commonly used in models that exhibit statically unstable behavior such as buckling [12,13]
- *viscous regularization* that is applied only to nodes on contact pairs that have just debonded. The viscous regularization damping causes the tangent stiffness matrix of the softening material to be positive for sufficiently small time increments. Viscous regularization damping is similar to the viscous regularization damping provided for cohesive elements and the concrete material model in Abaqus/Standard® [12,13].

Further details about the required input parameters are discussed in reference 8.

For automated propagation analysis, it was assumed that the computed behavior should closely match the benchmark results created below. For all analyses, the elastic constants and the input to define the fracture criterion were kept constant. Based on poor results in a previous investigation [3], automatic or static stabilization was not used in this study. Viscous regularization had yielded good results in the past [3,4], however, it was not used in the current study to limit the number of analyses. Instead, the study focused on using the default values and contact stabilization which had recently yielded good results [4]. This approach was used to gain confidence in the parameters that had been identified previously and thus determine if the selection of the parameters could be considered problem independent. Therefore, only the following items were varied to study the effect on the automated delamination propagation behavior during the analysis.

- The release tolerance (*reltol*) was varied.
- Analyses were performed with and without contact stabilization. For analyses that included contact stabilization only, a single stabilization factor (cs=1x10^{-6}) was used.
- Two- and three-dimensional models with different types of elements were used.

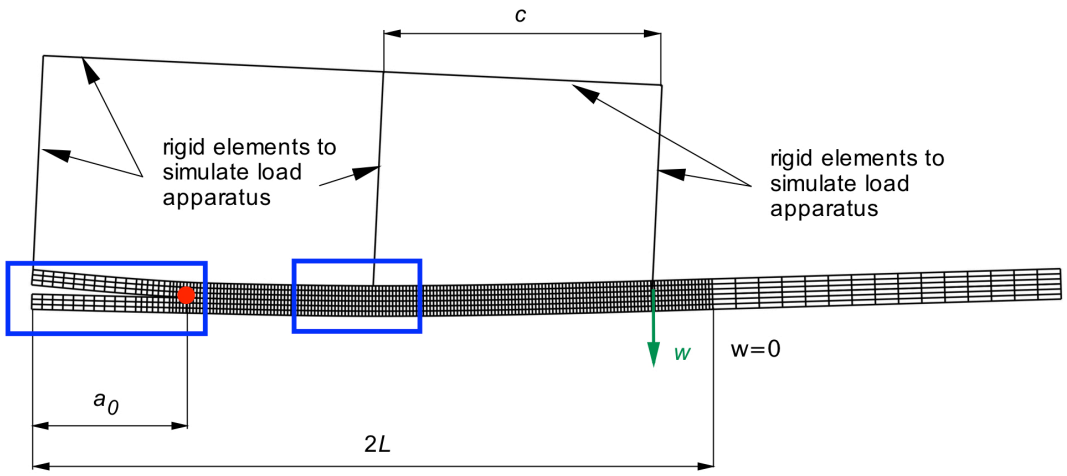

(a). *Mixed mode ratio G_{II}/G_T=0.5, c=41.3 mm.*

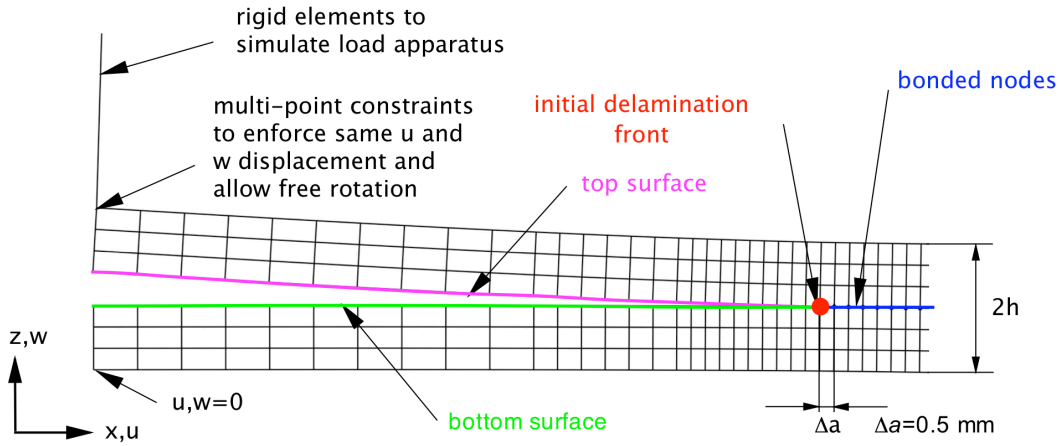

(b). *Detail of specimen tip and crack tip zone.*

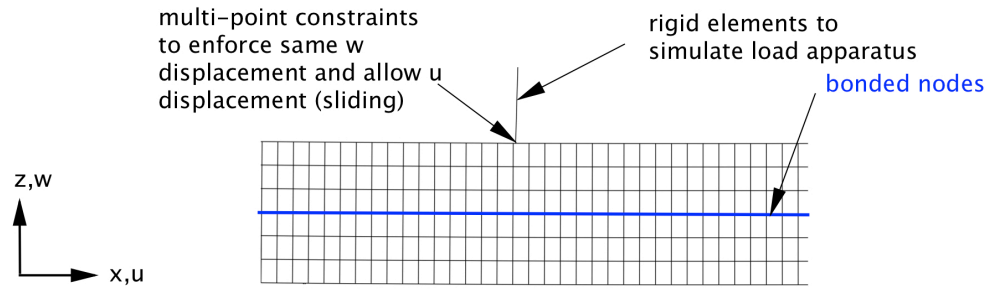

(c). *Detail of load introduction zone.*

Figure 3. *Deformed 2D FE-model of a MMB specimen.*

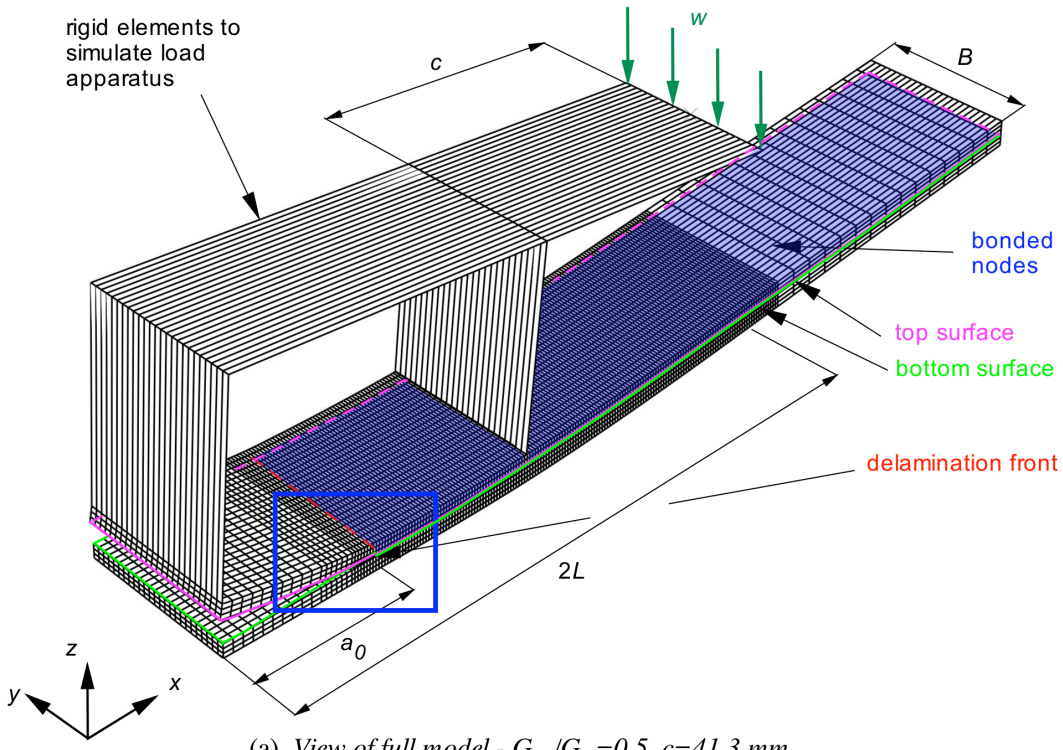

(a). *View of full model - G_{II}/G_T=0.5, c=41.3 mm.*

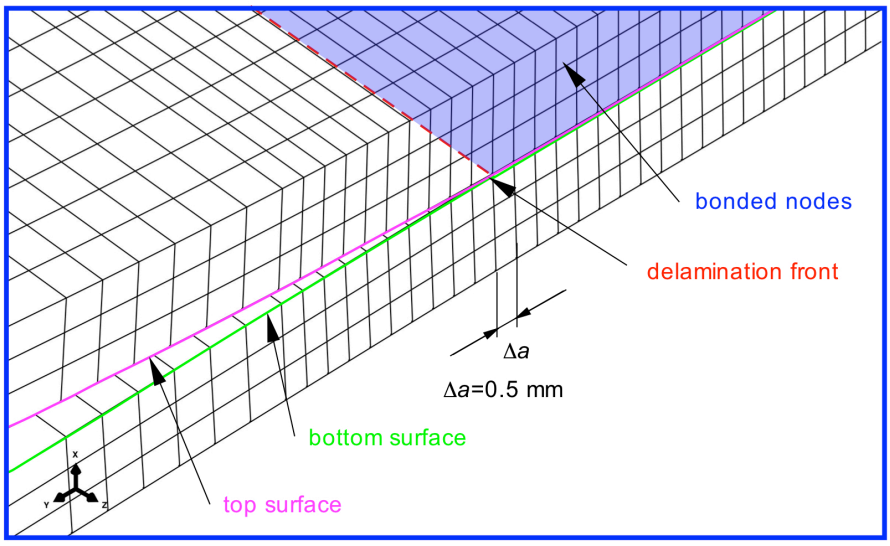

(b). *Detail of specimen tip and crack tip zone.*

Figure 4. *Deformed 3D FE-model of a MMB specimen.*

DEVELOPMENT OF THE STATIC BENCHMARK CASE

The static benchmark case was created based on the approach developed earlier [3]. Two-dimensional finite element models simulating MMB specimens with 16 different delamination lengths a_0 were created (25.4 mm$\leq a_0 \leq$70.6 mm). For each delamination length modeled, the load, P, and displacement, w, were monitored as shown in

Figure 5 (colored lines) for the case of 50% mode II (G_{II}/G_T =0.5). Using VCCT, the total strain energy release rate, G_T, and the mixed-mode ratio G_{II}/G_T were computed at the end of the analysis as shown in Figure 5. The failure index G_T/G_c was calculated by correlating the computed total energy release rate, G_T, with the mixed-mode fracture toughness, G_c, of the graphite/epoxy material. It is assumed that the delamination propagates when the failure index G_T/G_c reaches unity. Therefore, the critical load, P_{crit}, and critical displacement, w_{crit}, can be calculated for each delamination length modeled as discussed in detail in reference 7. The results were included in the load/displacement plots as shown in Figure 5.

These critical load/displacement results indicated that, with increasing delamination length, less load is required to extend the delamination up to a_0 ≈48 mm. To further extend the delamination, an increase in load is required past w=2.0 mm. For the first three delamination lengths, a_0, plotted in Figure 5, the values of the critical displacements also decreased at the same time. This means that the MMB specimen exhibits unstable delamination propagation under load control as well as displacement control in this region for G_{II}/G_T =0.5. The remaining critical load/displacement results indicated stable propagation. From these critical load/displacement results (solid grey circles and dashed line), two benchmark solutions can be created as shown in Figure 6. During the analysis, either prescribed displacements, w, or nodal point loads, P, are applied. For the case of prescribed displacements, w, (dashed blue line), the applied displacement must be held constant over several increments once the critical point (P_{crit}, w_{crit}) is reached, and the delamination front is advanced during these increments. Once the critical path (dashed grey line) is reached, the applied displacement is increased again incrementally. For the case of applied nodal point loads (dashed red line), the applied load must be held constant while the delamination front is advanced during these increments. Once the critical path (dashed grey line) is reached, the applied load is increased again incrementally.

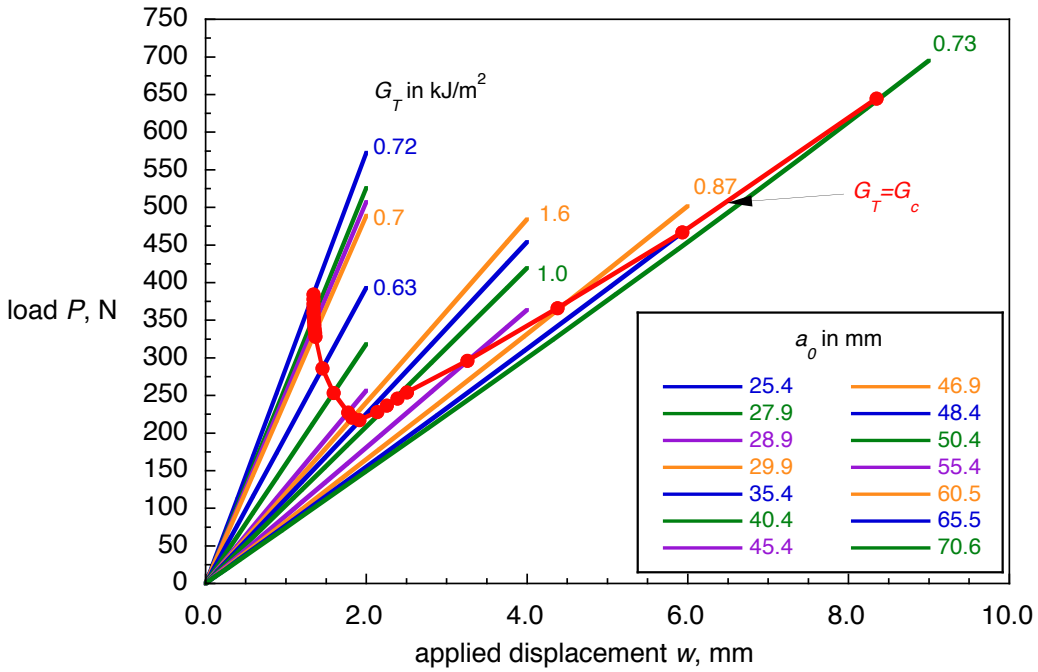

Figure 5. *Calculated critical load-displacement behavior for a MMB specimen.*

The benchmark result for prescribed displacements may also be visualized by plotting the prescribed displacements, w, at delamination growth onset versus the increase in delamination length, a^*, as illustrated in Figure 7. For the case of applied nodal point loads, the benchmark result may be visualized by plotting the applied loads, P, at delamination growth onset versus the increase in delamination length, a^*, as illustrated in Figure 8.

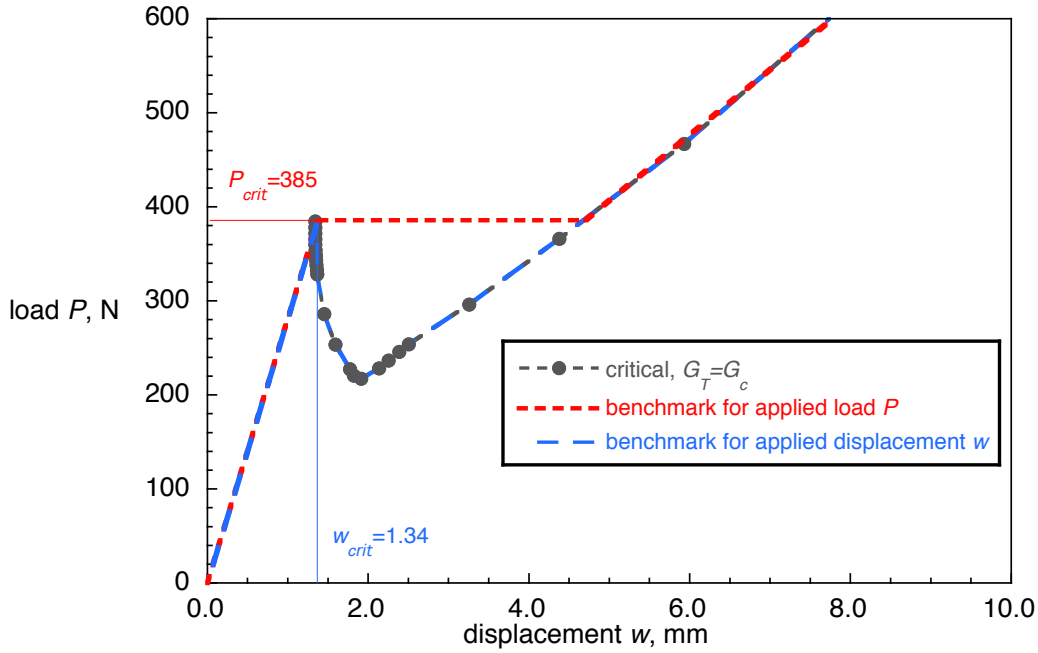

Figure 6. *Benchmark cases for applied load, P, and displacement, w.*

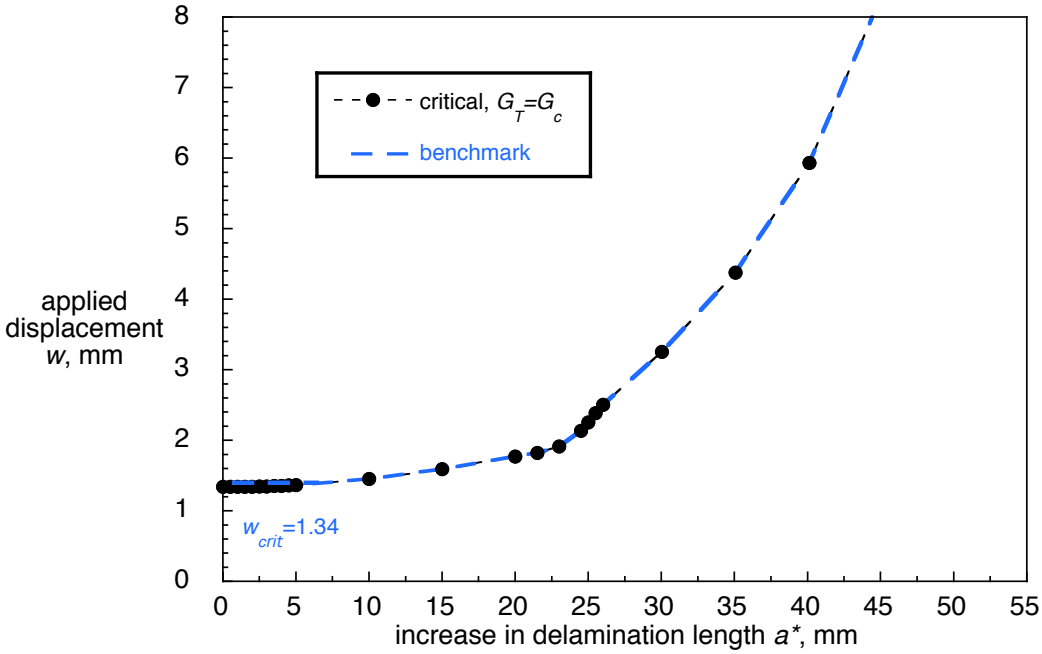

Figure 7. *Benchmark case for applied displacement, w.*

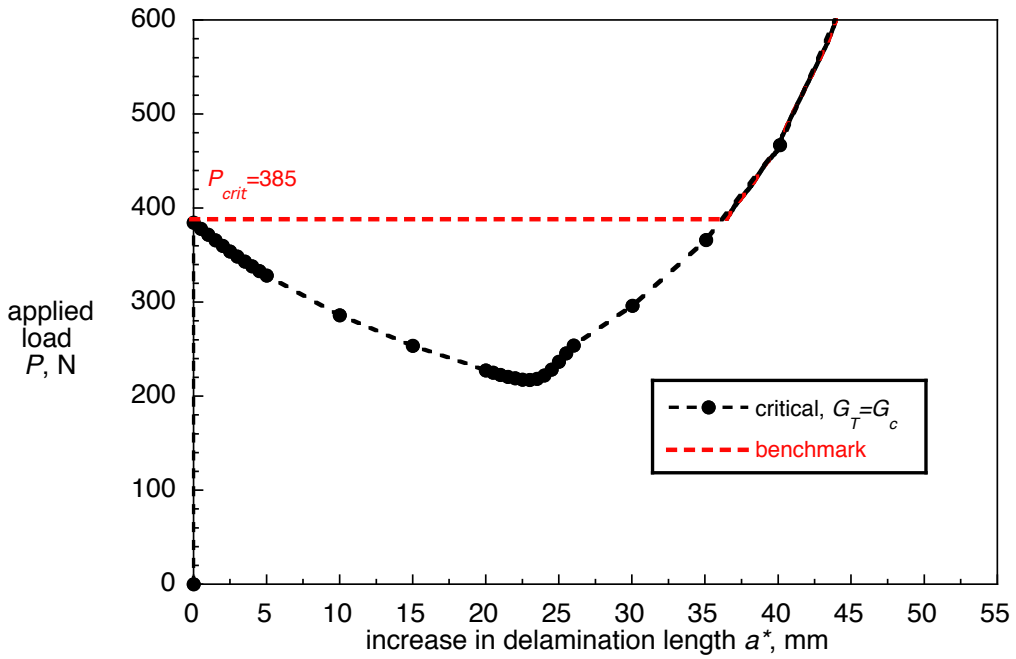

Figure 8. *Benchmark case for applied load, P.*

This way of presenting the results may be of advantage for large structures where local delamination propagation may have little effect on the global stiffness of the structure and may therefore not be visible in a global load/displacement plot. However, extracting the delamination length a from the finite element results required more manual, time consuming, post-processing of the results compared to the relatively simple and readily available output of nodal displacements and forces. The load/displacement, load/delamination-length or applied displacement/delamination-length relationship computed during automatic propagation should closely match the benchmark cases.

RESULTS FROM AUTOMATED PROPAGATION ANALYSIS

Computed delamination propagation for applied displacement

The propagation analysis was performed in two steps using the models shown in Figures 3a and 4a starting from an initial delamination length, a_0=25.4 mm. In the first step, a displacement of w=1.2 mm was applied which nearly equaled the critical displacement, w_{crit}=1.34 mm, determined earlier. In the second step, the applied displacement was increased to w=8.0 mm. For this second step, automatic incrementation was used in Abaqus/Standard® and a small increment size (0.5% of the total step) was chosen at the beginning of the step. To avoid termination, the analysis was allowed to cut back to an increment size of 10^{-18} of the total step. The analysis was limited to 5000 increments. Further details are discussed in reference 7.

Initially, analyses were performed using two-dimensional planar models (shown in Figure 3a) without stabilization or viscous regularization. Release tolerance values equal to the default value (*reltol*=0.2) [11] and smaller were used since these values

had yielded better results in the past [3,4]. Using the default value (*reltol*=0.2), the computed load and displacement exceeded the critical point before the initial load drop occurred and delamination propagation started (solid green line) as shown in Figure 9 where the computed resultant force (load *P*) is plotted versus the applied displacement *w*. The computed path initially stayed above the benchmark, however, as the displacement continued to increase over 2.5 mm, the computed load/displacement path converged to the benchmark result (solid grey circles and dashed grey line). To reduce the observed overshoot, the release tolerance was decreased. For a release tolerance *reltol*=0.1, the overshoot was reduced and the results improved (solid blue line) and shifted towards the benchmark case. For a release tolerance *reltol*=0.01, the analysis terminated once the critical point was reached (solid red line) due to convergence problems.

Based on problems identified during previous analyses, automated or static stabilization was not used in this study [3]. The results computed when contact stabilization (*cs*) was added are plotted in Figure 10. Using a stabilization factor of $cs=1x10^{-6}$, and a release tolerance (*reltol*=0.01) yielded results that were in excellent agreement with the benchmark (solid red line). Due to the fine mesh, only a small saw-tooth pattern was observed. The result confirms previous observations where small release tolerance values (*reltol*=0.01) in conjunction with a stabilization factor of $cs=1x10^{-6}$ had yielded excellent agreement with the benchmark results [3,4].

An alternative way to plot the benchmark is shown in Figure 11 where the applied displacement *w* is plotted versus the increase in delamination length *a**. The results plotted in Figure 11 are the examples that were discussed above and were shown in the global load/displacement plots of Figures 9 and 10. The conclusions that can be drawn from this plot are identical to those discussed above.

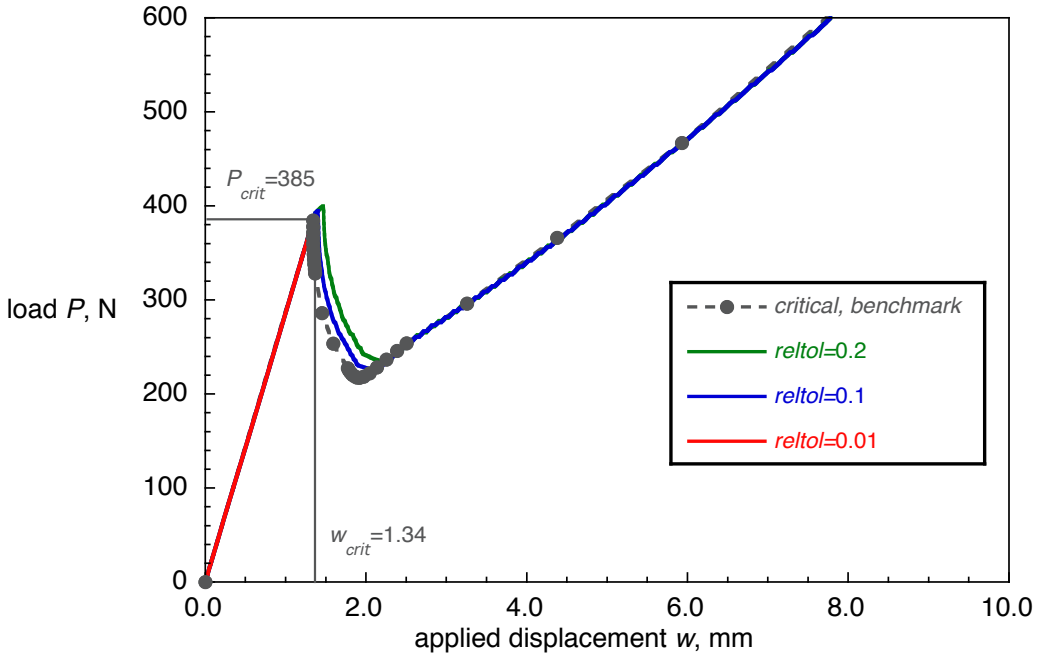

Figure 9. *Computed critical load-displacement behavior obtained from 2D planar models (CPE4) with different release tolerance settings.*

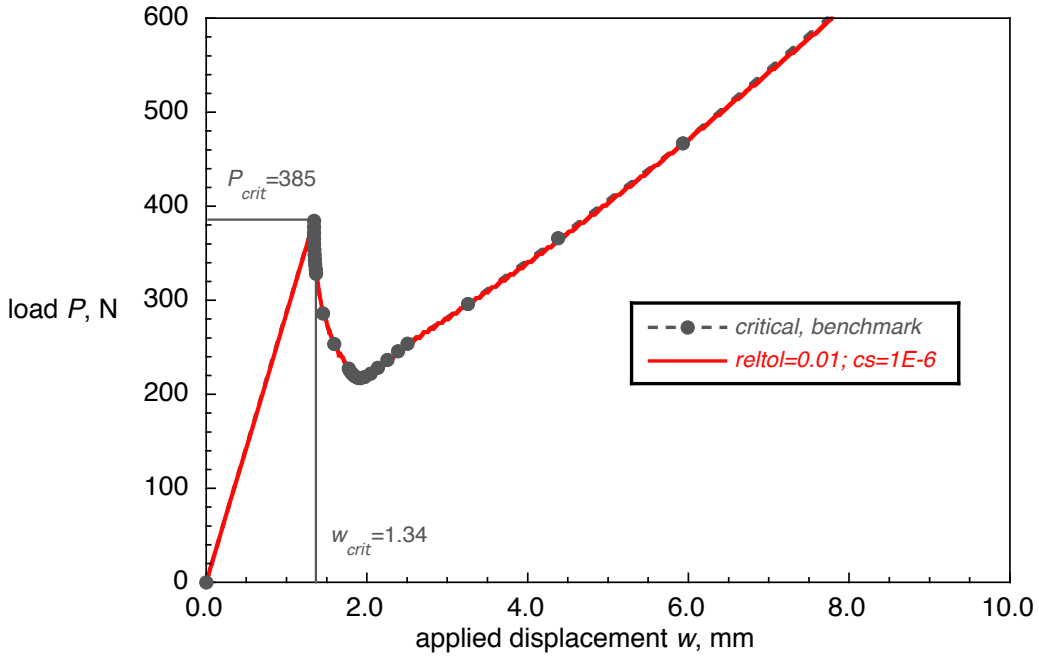

Figure 10. *Computed critical load-displacement behavior obtained from 2D planar models (CPE4) with added contact stabilization.*

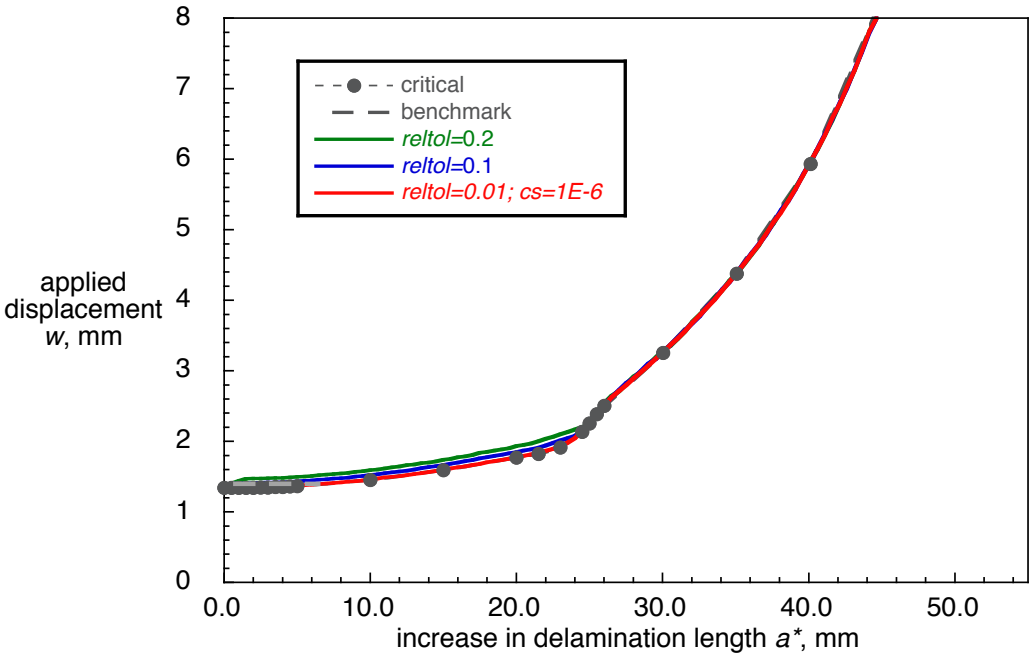

Figure 11. *Computed critical displacement-propagation behavior obtained from 2D planar models (CPE4).*

The result obtained from a three-dimensional analysis is shown in Figure 12. Based on the results from two-dimensional planar models shown above, contact stabilization was added to the analysis to help overcome convergence issues. Since the computer time increases with tighter release tolerances, a tolerance value (*reltol*=0.1) was selected.

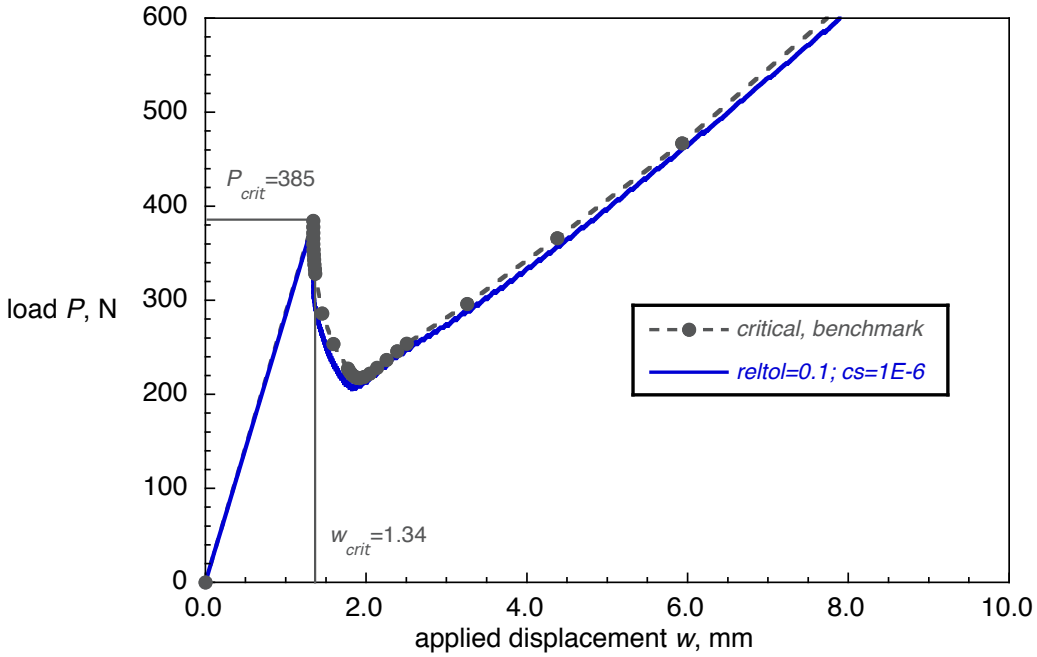

Figure 12. *Computed critical load-displacement behavior obtained from 3D solid models (C3D8I).*

The result (solid blue line) computed for a release tolerance value *reltol*=0.1 and a small stabilization factor $cs=1\text{x}10^{-6}$ are plotted in Figure 12. The load dropped and delamination propagation started upon reaching the critical point of the benchmark solution (solid circles and dashed grey line). The load/displacement path then ran parallel to the benchmark result but was shifted slightly towards lower loads. Deviation from the benchmark may be explained by the fact that the benchmark results were created using two-dimensional planar finite element models of the MMB specimen. Three-dimensional models, which provide a better approximation of reality, however, yield a failure index that is somewhat higher across the entire width than the results from two-dimensional planar finite element models as discussed in detail in reference 7. Therefore, delamination propagation is expected to start prior to the benchmark results obtained from two-dimensional planar finite element analysis, which ultimately leads to a shift of the entire results plot towards lower loads.

Computed delamination propagation for applied quasi-static load

The propagation analysis was performed in two steps using the models shown in Figures 3a and 4a starting from an initial delamination length, a_0=25.4 mm. In the first step, a load P=360 N was applied which equaled nearly the critical load, P_{crit}=385 N, determined earlier. In the second step, the total load was increased (P=600 N). The settings for incrementation were identical to the values mentioned in the section on applied displacements.

The same steps discussed in the section on applied displacement were followed. Initially, analyses were performed using two-dimensional planar models without stabilization or viscous regularization. For the default value of *reltol*=0.2, the load stopped increasing after reaching the critical point, but the analysis terminated immediately (solid green line) due to convergence problems as shown in Figure 13.

The release tolerance was not increased as suggested by the Abaqus/Standard® error in the message (.msg) file. Previous analysis had shown that, by increasing the release tolerance (*reltol*>0.2), termination of the analysis could be avoided. However, the results had not been in good agreement with the benchmark [3,4]. Therefore, additional stabilization had to be introduced in order to obtain agreement with the benchmark case.

The results computed when contact stabilization (*cs*) was added are plotted in Figure 14. A small stabilization factor (*cs*=1x10^{-6}) was used for all cases since it had yielded good results in previous analyses [3, 4]. Initially, the release tolerance value was set at the default value (*reltol*=0.2) (solid green line). For this parameter combination, the load increased up to the critical point, and delamination propagation started while the load remained constant (solid green line). Also for the stable propagation path, the result was in good agreement with the benchmark result (solid grey line). Then, the release tolerance was reduced to *reltol*=0.1 (solid blue line) and further to *reltol*=0.01 (solid red line). For all cases, the results were in good agreement with the benchmark results over the entire load/displacement range.

An alternative way to plot the benchmark is shown in Figure 15 where the applied load *P* is plotted versus the increase in delamination length *a**. The results plotted in Figure 15 are the same as those that were discussed above and were shown as global load/displacement plots in Figure 14. The conclusions that can be drawn from the plots in Figure 15 are identical to those discussed in the above for Figure 14.

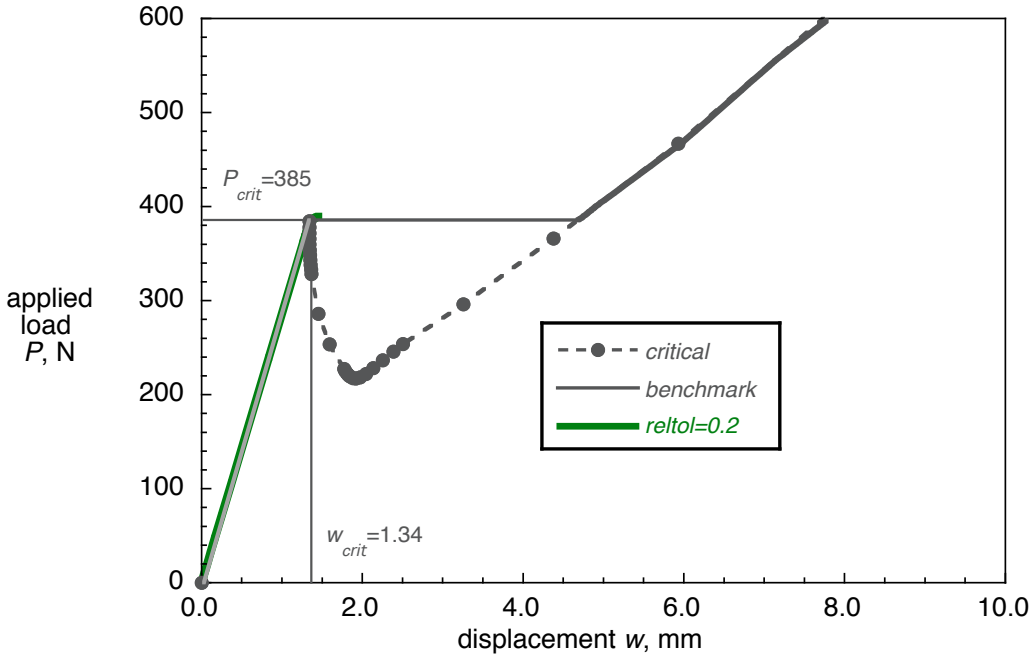

Figure 13. *Computed critical load-displacement behavior obtained from 2D planar models (CPE4I) with different release tolerance settings.*

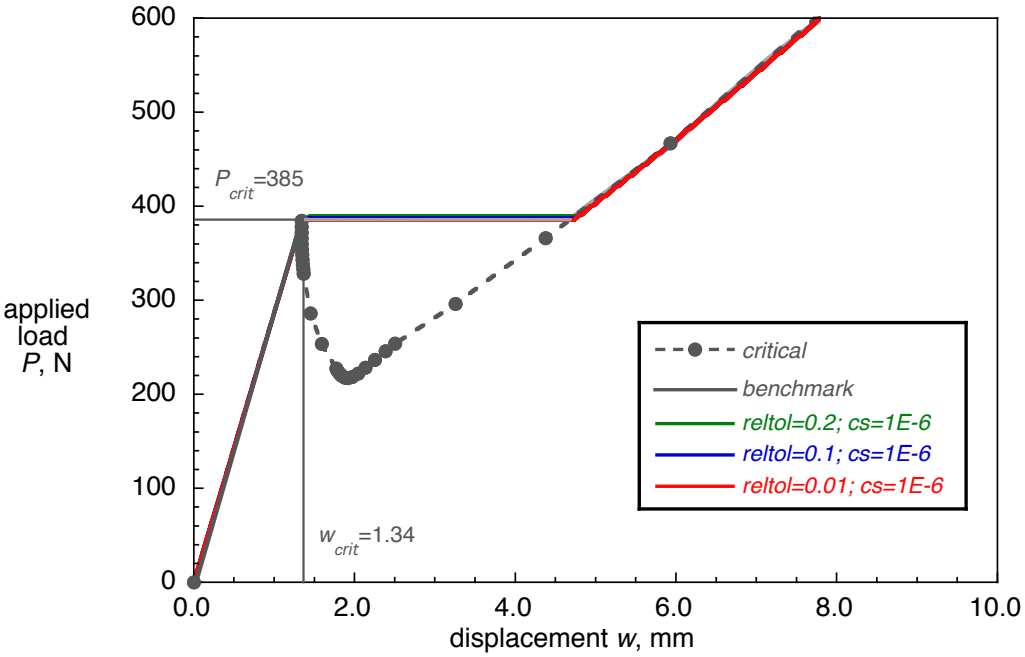

Figure 14. *Computed critical load-displacement behavior obtained from 2D planar models (CPE4I) with added contact stabilization.*

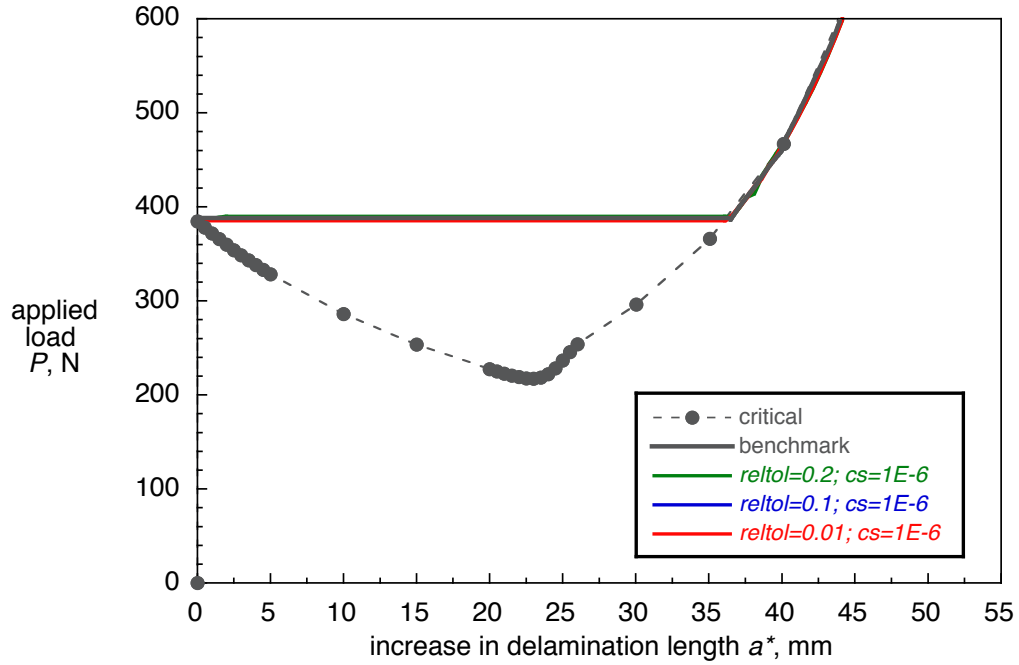

Figure 15. *Computed critical load-propagation behavior obtained from 2D planar models (CPE4I).*

A result obtained from a three-dimensional model is shown in Figure 16. Based on the results from two-dimensional planar models shown above, contact stabilization was added to help overcome convergence issues. A release tolerance value (*reltol*=0.1) was used which had yielded good results previously. The load/displacement result computed when a small stabilization factor (cs=1x10^{-6}) was added is plotted in Figure 16.

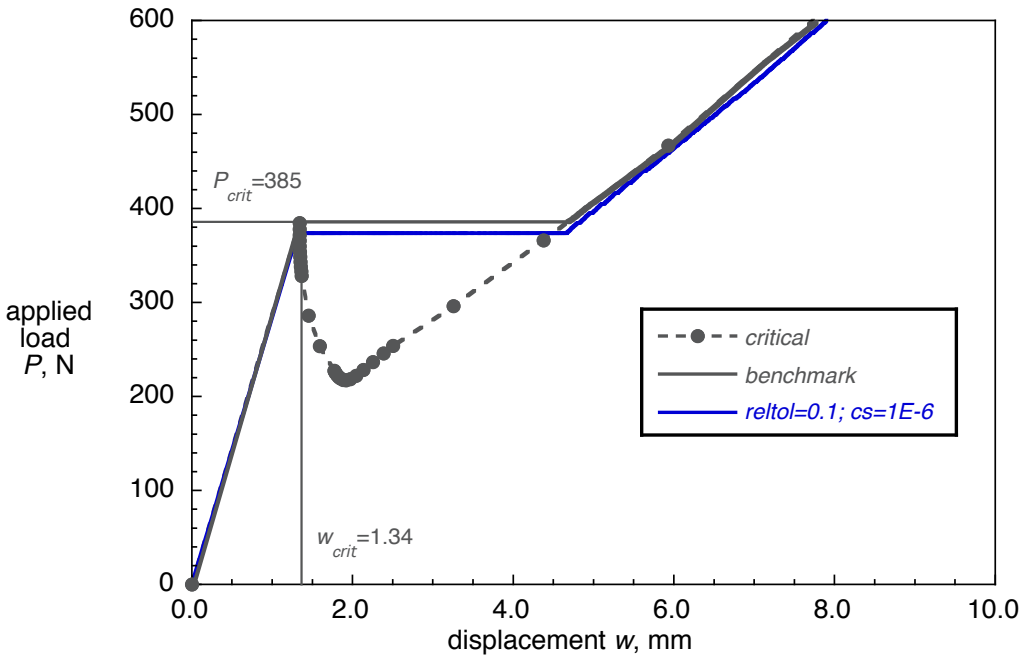

Figure 16. *Computed critical load-displacement behavior obtained from 3D solid models (C3D8I).*

The load increase stopped and delamination propagation started (solid blue line) shortly before reaching the critical point of the benchmark solution (solid grey line). As mentioned earlier and discussed in detail in reference 7, deviation from the benchmark may be explained by the fact that the benchmark results were created using two-dimensional planar finite element models of the MMB specimen.

SUMMARY AND CONCLUSIONS

The development of a benchmark example, which allows the assessment of the static delamination propagation prediction capabilities was presented and demonstrated for Abaqus/Standard®. The example is based on finite element models of the mixed-mode I/II Mixed-Mode Bending (MMB) specimen for 50% mode II. The models are independent of the analysis software used and allow the assessment of the automated delamination growth prediction capabilities in commercial finite element codes based on the virtual crack closure technique (VCCT).

First, a quasi-static benchmark result was created based on the approach developed in reference 3. Two-dimensional finite element models were used for simulating the MMB specimen with 50% mode II and different initial delamination lengths, a_0. For each delamination length modeled, the load and displacements were monitored. The mixed-mode I/II strain energy release rate was calculated for a fixed applied displacement. The delamination was assumed to propagate when the total strain energy release rate reached the fracture toughness value. Thus, critical loads and critical displacements for delamination propagation were calculated for each initial delamination length modeled. From these critical load/displacement results,

benchmark solutions were created. The load/displacement relationship computed during automatic propagation should closely match the benchmark cases.

After creating the benchmark cases, the approach was demonstrated for the commercial finite element code Abaqus/Standard®. Starting from an initially straight front, the delamination was allowed to propagate under quasi-static loading based on the algorithms implemented into the software. Input control parameters were varied to study the effect on the computed delamination propagation and growth.

The results showed the following:

- The benchmarking procedure proved valuable by highlighting the issues associated with choosing the input parameters of the particular implementation.
- In general, good agreement between the results obtained from the automated propagation analysis and the benchmark results could be achieved by selecting input parameters that had previously been determined during analyses of mode I Double Cantilever Beam and mode II End Notched Flexure specimens.
- In particular, the results for automated delamination propagation analysis under quasi-static loading showed the following:
    - Using the default release tolerance (*reltol*=0.2) as suggested in the Abaqus/Standard® handbook or increasing the value, as suggested in the user's manual, may help to overcome convergence problems, however, it leads to an undesired overshoot of the computed result compared to the benchmark.
    - A combination of release tolerance and contact stabilization is required to obtain more accurate results.
    - A gradual reduction of the release tolerance and contact stabilization over several analyses is suggested.
    - Good agreement between analysis results and the benchmarks could be achieved for release tolerance values (*reltol*<0.1) in combination with contact stabilization (cs=1x10^{-6}).

Overall, the results are promising and the current findings concur with previously published conclusions [3,4,6]. However, further assessment for mixed-mode delamination fatigue onset and growth is required. Additional studies should also include the assessment of the propagation capabilities in more complex mixed-mode specimens and on a structural level.

Assessing the implementation in one particular finite element code illustrated the value of establishing benchmark solutions since each code requires specific input parameters unique to its implementation. Once the parameters have been identified, they may then be used as a starting point to model delamination growth for more complex configurations.

ACKLOWLEDGEMENTS

This research was supported by the Subsonic Rotary Wing Project as part of NASA's Fundamental Aeronautics Program.

The analyses were performed at the Durability, Damage Tolerance and Reliability Branch at NASA Langley Research Center, Hampton, Virginia, USA.

REFERENCES

1. E. F. Rybicki and M. F. Kanninen, "A Finite Element Calculation of Stress Intensity Factors by a Modified Crack Closure Integral," *Eng. Fracture Mech.,* Vol. 9, pp. 931-938, 1977.
2. R. Krueger, "Virtual Crack Closure Technique: History, Approach and Applications," *Applied Mechanics Reviews,* Vol. 57, pp. 109-143, 2004.
3. R. Krueger, "An Approach to Assess Delamination Propagation Simulation Capabilities in Commercial Finite Element Codes," NASA/TM-2008-215123, 2008.
4. R. Krueger, "Development and Application of Benchmark Examples for Mode II Static Delamination Propagation and Fatigue Growth Predictions," NASA/CR-2011-217305, NIA report no. 2011-02, 2011.
5. A. C. Orifici and R. Krueger, "Assessment of Static Delamination Propagation Capabilities in Commercial Finite Element Codes Using Benchmark Analysis," NASA/CR-2010-216709, NIA report no. 2010-03, 2010.
6. R. Krueger, "Development of a Benchmark Example for Delamination Fatigue Growth Prediction," NASA/CR-2010-216723, NIA report no. 2010-04, 2010.
7. R. Krueger, "Development and Application of Benchmark Examples for Mixed-Mode I/II Quasi-Static Delamination Propagation Predictions," NASA/CR-2012-217562, 2012.
8. I. S. Raju and T. K. O'Brien, "Fracture Mechanics Concepts, Stress Fields, Strain Energy Release Rates, Delamination and Growth Criteria," in *Delamination Behavior of Composites*, S. Sridharan, Ed.: Woodhead Publishing in Materials, 2008.
9. T. K. O'Brien, W. M. Johnston, and G. Toland, "Mode II Interlaminar Fracture Toughness and Fatigue Characterization of a Graphite Epoxy Composite Material," NASA/TM-2010-216838, 2010.
10. M. L. Benzeggagh and M. Kenane, "Measurement of Mixed-Mode Delamination Fracture Toughness of Unidirectional Glass/Epoxy Composites with Mixed-Mode Bending Apparatus," *Composites Science and Technology,* Vol. 56, pp. 439-449, 1996.
11. KaleidaGraph: Version 4.1, 2009.
12. *Abaqus Analysis User's Manual*, ABAQUS® Standard, Version 6.10, DSS Simulia, 2010.
13. *Abaqus Theory Manual*, ABAQUS® Standard, Version 6.10, DSS Simulia, 2010.